

having an average energy of 20 Mev then there will be at most 6×10^{27} protons stored. Now, isotopes produced in one locality will rather rapidly achieve a global distribution; thus we can treat these protons as if they are dumped uniformly over the surface of the earth. Thus some 10^9 protons will fall on each square centimeter of the top of the atmosphere. Even this number, which is certainly a gross overestimate, is one order of magnitude less than the number of solar particles brought in during a solar cycle, which are relatively ineffective in producing radioisotopes. Thus dumping of particles from the radiation belts are of negligible importance.

These results can be summarized as follows. The effect of removing the field is to increase the radiation dosage due to the cosmic radiation by 0 to 6 mrad/year between the polar regions and the equator and to increase that due to radioactive isotopes selectively taken up by organisms by not more than 2 mrad/year. These values are so small, particularly in comparison with the general background radiation levels always present, that it seems inconceivable that they could appreci-

ably affect the evolution of any organisms. The hypothesis that the additional energetic particle radiation allowed to fall on the earth when the geomagnetic field is reversed is the causative agency for population changes thus appears untenable unless it is assumed that these periods are associated with greatly increased particle radiation from some external source.

C. J. WADDINGTON

School of Physics and Astronomy,
University of Minnesota, Minneapolis

References and Notes

1. A. Cox, R. R. Doell, G. B. Dalrymple, *Science* **144**, 1537 (1964); R. R. Doell, G. B. Dalrymple, A. Cox, *J. Geophys. Res.* **71**, 531 (1966); I. McDougall and D. H. Tarling, *Nature* **200**, 54 (1963).
2. N. D. Opdyke, B. Glass, J. D. Hays, J. Foster, *Science* **154**, 349 (1966).
3. J. F. Simpson, *Geol. Soc. Amer. Bull.* **77**, 197 (1966).
4. R. J. Uffen, *Nature* **198**, 143 (1963).
5. D. Lal and B. Peters, *Handbuch der Physik*, **46/2**, 551 (1967).
6. Report of the United Nations Scientific Committee on the Effects of Atomic Radiation, General Assembly Official Records, 13th Session, Suppl. No. 17 (A/3838).
7. R. E. Lingenfelter, *Rev. Geophys.* **1**, 35 (1963).
8. R. E. Lingenfelter and E. J. Flamm, *J. Atmos. Sci.* **21**, 134 (1964).
9. J. D. Van Allen (Reidel, Dordrecht, Netherlands, 1966).
10. Supported by the Office of Naval Research under contract Nonr-710(60).

2 August 1967

Electron Microprobe and Optical Absorption Study of Colored Kyanites

Abstract. The characteristic blue color of the mineral kyanite is shown to be caused by traces of Ti^{+++} in the range of a few parts per million. Evidence from the intensity and position of optical absorption bands indicates that the unusually intense color probably arises from electron delocalization into narrow d-bands.

The mineral kyanite (Al_2SiO_5) quite often exhibits a characteristic blue color which has so far remained unexplained. The bright blue color plus its relatively great hardness have resulted in its use as a gemstone. In some of the mineralogical literature it is presumed that the color is due to ferric iron, although published analyses (1) indicate that a variety of transition elements are pres-

ent in small amounts, any one of which is a possible chromophore. The problem is intriguing, because the trace element content varies rather widely among specimens from different localities and yet the blue color is almost a hallmark of naturally occurring kyanite.

We have used a combination of electron microprobe, absorption spectroscopy, and emission spectroscopy to

demonstrate that the color arises from very small amounts of trivalent titanium substituting for aluminum in the kyanite structure. The titanium is usually in concentrations in the range of 20 to 50 parts per million and at that concentration has an absorption that dominates the absorption of other impurity elements which may be present at the fractional percent level. The intensity and band positions in the absorption spectrum further indicate that the single d-electron of the Ti^{+++} is delocalized and that the absorption process can best be explained by a narrow d-band model.

Kyanites from six localities were selected. Five of these were the characteristic blue kyanites and the sixth (Brazilian) was a transparent pale green crystal with a few blue patches. All specimens were analyzed for bulk trace element content by emission spectroscopic techniques. Polished sections were prepared for microprobe examination and oriented polished slices of the India and the Brazilian kyanites were prepared for the optical absorption measurements.

The electron microprobe was operated at 30 keV and 0.20 μa , with a 10- μ spot size and a 52° take-off angle. Calibrations were made by using pure metal standards and a specimen current of 0.005 μa . The x-ray count data were corrected for background but were not corrected for effects of absorption and so forth, so that reported concentrations may be in error by up to ± 20 percent of the measured amount. Optical absorption spectra were recorded in transmission on a Beckmann DK-2A spectrophotometer. A matched pair of Glan prisms were used to measure the polarized spectra. The emission spectrographic analyses were made by use of external standards. The analyses are semiquantitative, being good to about ± 50 percent of the amount present (2).

Table 1 summarizes the emission spectrographic and electron microprobe

Table 1. Semiquantitative emission spectrographic (Spec.) and electron microprobe (E.P.) analyses of kyanite. Results are in parts per million. ND, not detected. Sought but not detected: B, Cu, Ag, Zn, Co, Ni, Mo, Sn, Pb, Ge, In, Sb, Cd, Bi, Y, Yb, Sr, Ba.

Element	Chesterfield, Mass.		Litchfield, Conn.		Whitehorse, Pa.		Zillerthal, Tyrol		India (Placer)		Brazil (Green)	Brazil (Blue)
	Spec.	E.P.	Spec.	E.P.	Spec.	E.P.	Spec.	E.P.	Spec.	E.P.	E.P.	E.P.
Fe	1000	900	1000	1000	1500	1000	5000	5600	1500	800	9000	7000
Cr	50	150	150	20	50	70	ND	ND	150	100	ND	ND
V	200	100	200	90	200	100	200	100	100	200	60	60
Ti	60	20	80	270	100	1200	100	70	40	90	10	60
Mn	ND		ND		ND		ND		ND		100	100

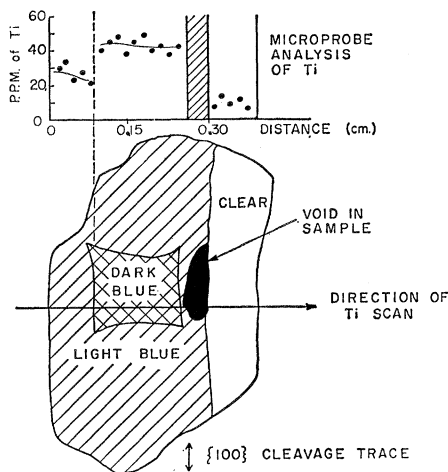


Fig. 1. Variation in titanium content across a polished kyanite crystal with blue patches of various color depth.

analyses of the six samples. The impurities of interest are iron, vanadium, chromium, and titanium. Manganese was found only in the Brazilian specimen. Differences between the emission spectrographic and electron probe analyses are expected because of different sources of instrumental error, slightly different samples being used for analysis, and in the case of iron, spectrographic analyses tend to be high because of included impurities in the bulk. These elements, except titanium, were all quite uniformly distributed within each crystal, thus showing no correlation with the patchy nature of the blue color. The titanium ranges from 10 to 1200 parts per million, with the highest concentration in a very dark blue portion of the Whitehorse kyanite. That the blue color is related to the titanium concentration is shown in Fig. 1. The set of analyses across a polished section of an India kyanite shows the correlation of titanium concentration with density of the blue color. The titanium concentration needed to generate a deep blue color is only about 50 parts per million (ppm). It is interesting to note that, although the electron microprobe is not usually considered to be a trace element tool, it is possible to measure titanium concentrations as low as 10 parts per million in an alumina silicate matrix.

All samples, except the Zillerthal and Brazil specimens, exhibited a bright red to violet cathodoluminescence which is believed to be caused by Cr^{+++} . This belief is reinforced by the similarity of the luminescence to that of ruby and by the fact that it is absent in the two samples that have no detectable chromium.

The optical absorption spectrum of a blue Indian kyanite is shown in Fig. 2. All three polarization directions show a single band at $16,670\text{ cm}^{-1}$ with an unresolved shoulder at $13,000\text{ cm}^{-1}$. A single band is expected from Ti^{+++} whereas a two- or three-band spectrum would be expected from V^{+++} or Cr^{+++} (3). The splitting of the band could be due either to the low symmetry of the Al^{+++} site in kyanite (4) or to a Jahn-Teller splitting (3). In contrast, the spectrum of the green Brazilian kyanite (Fig. 3) is that expected of ferric iron. An iron concentration of 0.9 percent by weight is required to produce the observed intensity. The three bands at 9300 , $16,400$ and $22,700$ (doublet) cm^{-1} may be compared with the Fe^{+++} ${}^6\text{A}_{1g} \rightarrow {}^4\text{T}_{1g}$, ${}^4\text{T}_{2g}$, and $({}^4\text{A}_{1g}, {}^4\text{E}_g)$ transitions measured by Dvir and Low (5) on Fe^{+++} in beryl. The 9300 cm^{-1} band is lower than the $14,200\text{ cm}^{-1}$ band in beryl but the two higher transitions agree fairly well. The agreement between the $16,400\text{ cm}^{-1}$ Fe^{+++} band and the $16,670\text{ cm}^{-1}$ Ti^{+++} band is accidental, although it is possible that traces of Ti^{+++} contribute to the intensity.

The blue color of the Indian kyanite can be bleached by heating the crystals in air at 1200°C , although the reaction proceeds very slowly and bleaching is not complete in 24 hours.

We turn now to an explanation for the unusually intense absorption of Ti^{+++} which allows this chromophore to dominate all other absorbing ions and thus generate a ubiquitous blue color. The extinction coefficient of the band in Fig. 2 is $1200\text{ mole liter}^{-1}\text{ cm}^{-1}$, which is rather too intense for a crystal field transition [compare with the value of $3\text{ mole liter}^{-1}\text{ cm}^{-1}$ observed by Holmes and McClure (6) for Ti^{+++} in $\text{CsTi}(\text{SO}_4)_2 \cdot 12\text{H}_2\text{O}$]. Crystal field bands of ions on noncentrosymmetric sites have a higher intensity [compare $25\text{ mole liter}^{-1}\text{ cm}^{-1}$ for Fe^{++} on the highly distorted M_2 site in orthopyroxene (7)] but the distortions of the alumina octahedra in kyanite are not extreme and some further contribution to the intensity seems necessary. An additional difficulty is that although the band shape of the Ti^{+++} band is that characteristic of a d-d transition, the frequency of $16,670\text{ cm}^{-1}$ is much lower than the $20,300\text{ cm}^{-1}$ reported for the titanium alum and for $\text{Ti}^{+++}:\text{Al}_2\text{O}_3$ (8). Yet the Al^{+++} sites in kyanite are smaller than a normal Ti^{+++} site which should increase rather than decrease the transition energy. The possibility that

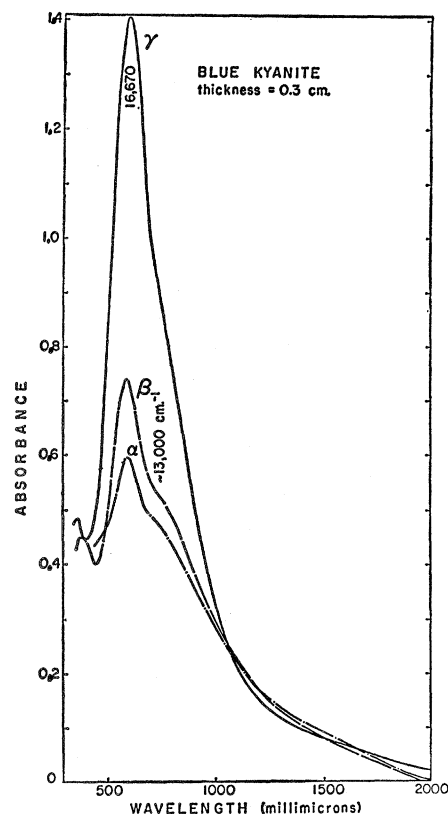


Fig. 2. Optical absorption spectrum of Ti^{+++} in a blue Indian kyanite for light polarized along each of the vibration directions.

the color arises from Ti^{+++} on the tetrahedral Si^{4+} sites can be ruled out from crystal chemical considerations and from the frequency of the absorption band.

One possibility is that the blue color of kyanite is analogous to the intense blue color observed in slightly reduced rutile (9) and in the other intermediate

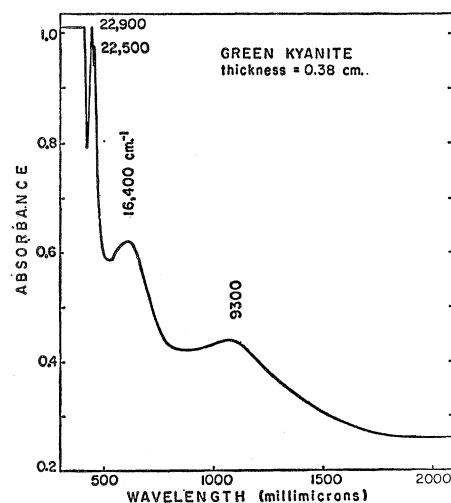


Fig. 3. Unpolarized optical absorption spectrum of Fe^{+++} in a light green Brazilian kyanite.

oxides of titanium (10). The intense absorption spectra of these oxides can be explained by the model of narrow d-bands formed by d-orbital overlap proposed by Goodenough (11). The t_{2g} ground state orbitals overlap directly across shared faces in the case of Ti_2O_3 and through the intermediary of the oxygen p -orbitals in the case of TiO_2 . The narrow bands thus formed lie within the forbidden energy gap of the structures.

The spectra of transparent kyanite crystals show no features below 40,000 cm^{-1} , so the Ti^{+++} absorption lies well within the forbidden gap. The aluminum-oxygen octahedra in kyanite are arranged with shared edges forming chains parallel to the c -axis (4). The closest aluminum-aluminum distances along the main chain are 2.79 Å, which may be compared with the titanium-titanium edge-sharing distance in Ti_2O_3 of 2.79 Å (12). This distance is less than the critical separation required for one lobe of the t_{2g} ground state orbital to overlap an adjacent orbital to form a narrow band. Since the concentration of Ti^{+++} in kyanite is very low, this model further requires that the Ti^{+++} ions be clustered to permit a sufficient number of Ti^{+++} cation neighbors for collective electron behavior.

EUGENE W. WHITE
WILLIAM B. WHITE

Materials Research Laboratory,
Pennsylvania State University,
University Park 16802

References and Notes

1. W. A. Deer, R. A. Howie, J. Zussman, *Rock Forming Minerals* (Wiley, New York, 1962), vol. 1, p. 140.
2. Emission spectrographic analyses were done by N. Suhr of the Mineral Constitution Laboratory at Pennsylvania State University.
3. D. S. McClure, *J. Chem. Phys.* **36**, 3757 (1962).
4. C. W. Burnham, *Z. Krist.* **118**, 337 (1963).
5. M. Dvir and W. Low, *Phys. Rev.* **119**, 1587 (1960).
6. O. G. Holmes and D. S. McClure, *J. Chem. Phys.* **26**, 1686 (1957).
7. G. M. Bancroft and R. G. Burns, *Am. Mineralogist*, in press.
8. The frequency of the ${}^2T_{2g} \rightarrow {}^2E_g$ transition of Ti^{+++} in the corundum structure seems uncertain. McClure (ref. 3) measured a value of 20,300 cm^{-1} on a flame-grown boule with a titanium content of about 0.2 mole percent. We found a value of 17,500 cm^{-1} in a star sapphire with 0.5 percent titanium, which is in better agreement with the value found in kyanite.
9. D. C. Cronmeyer, *Phys. Rev.* **113**, 1222 (1959).
10. V. R. Porter, W. B. White, R. Roy, *Am. Ceram. Soc. Bull.* **45**, 810 (1966).
11. J. B. Goodenough, *Magnetism and the Chemical Bond* (Wiley, New York, 1963); *Bull. Soc. Chim. France* **1965**, 1200 (1965); *Materials Res. Bull.* **2**, 37, 165 (1967).
12. R. E. Newnham and Y. M. DeHaan, *Z. Krist.* **117**, 235 (1962).
13. Supported by the Advanced Research Projects Agency under contract No. DA-49-083.

23 August 1967

Sedimentary Phosphate Method for Estimating Paleosalinities

Abstract. *The widespread occurrence of sedimentary phosphate in argillaceous sediments provides the basis for a new method of paleosalinity estimation. Sedimentary phosphate contains iron- and calcium-phosphate fractions, the relative proportions of which are sensitive to salinity of the water at sites of deposition. The sedimentary phosphate method provides direct estimates of paleosalinity throughout the freshwater to marine range.*

Recently great efforts have been made to develop geochemical techniques to estimate environmental parameters such as temperature and salinity. While the oxygen isotope method for paleotemperatures (1) has been employed extensively, efforts to refine methods for paleosalinities have been less successful. Most paleosalinity methods are based on Goldschmidt's (2) classical observations on the occurrence and distribution of trace elements in different sedimentary environments. For example, DeGENS *et al.* (3) differentiated marine from freshwater shales on the basis of spectrochemical analysis for boron, gallium, and rubidium. Similarly, POTTER *et al.* (4) demonstrated that each of the elements boron, chromium, copper, nickel, and vanadium is more abundant in marine than in freshwater argillaceous sediments. The utility of trace element paleosalinity indicators as employed by such authors is limited, because the absolute abundance of an element in a sediment sample depends upon the trace element content of the detrital minerals, grain size, mineral composition, organic content, sedimentation rate, and so forth, as well as upon salinity of the water at the site of deposition. Therefore, the abundance data for a particular environment cluster around a mean value, but there is sufficient spread that significant distinctions cannot be made between environments that differ by small increments in salinity.

Most recent research has concentrated on developing the single element boron method for paleosalinity determination (5). Several studies have tested the conditions required for the boron method to be a useful indicator (6). The results to date (7) indicate that when the whole-rock boron is below 50 parts per million the sample probably is freshwater in origin, while a boron content above 50 parts per million suggests marine conditions. It appears that only a general distinction between freshwater and marine sediments can be made. The several factors that control the abundance of boron mask the sensitivity of the method to

all but the extreme environmental salinity variations. The absolute abundance depends on the boron content of the detrital sediment, as well as upon conditions in the depositional basin. Furthermore, the conditions leading to boron adsorption in the depositional environment are imperfectly known (8). It appears that a sensitive and generally applicable method of paleosalinity estimation will have to be based on a new principle. It is the purpose of this paper to propose such an alternative.

The new method is based on the discovery that both recent and ancient argillaceous sediments contain small quantities of sedimentary phosphate that are distributed widely in sediments from different environments. The sedimentary phosphate can be extracted selectively from the sediment and differentiated into fractions whose relative proportions are sensitive to the salinity of the water at the site of deposition. The phosphate fractions are interdependent variables affected by salinity. The ratio between them is independent of their absolute abundance in the sediment and many of the difficulties inherent in the methods discussed above are avoided. For convenience, the new method of estimating paleosalinities is called the Sedimentary Phosphate Method.

Compared to the small concentrations found in natural waters, relatively large amounts of phosphorus occur in sediments. Sediments act as a phosphorus reservoir in natural systems. Mortimer's (9) classic study of lakes demonstrated that phosphorus is associated with iron in lake sediments and that under certain conditions it is released to the lake water. Similarly, there is exchange between water and the sediment reservoir in estuarine and marine environments (10). The mineral or chemical composition of the phosphorous compounds in estuarine and marine sediments has not been determined, although it is well known that marine phosphorite is essentially $Ca_{10}(PO_4)_5(CO_3)(F,OH)_2$. The objective of the present study was to characterize the types of sediment phosphorus that exist over a range of